Adsorbate-Induced Changes in the Surface Composition of Bimetallic Clusters: Pt−Au on TiO2(110)

ARTICLE *in* THE JOURNAL OF PHYSICAL CHEMISTRY C · NOVEMBER 2010

Impact Factor: 4.77 · DOI: 10.1021/jp108939h

7 AUTHORS, INCLUDING:

Salai Cheettu Ammal
University of South Carolina
55 PUBLICATIONS **799** CITATIONS
SEE PROFILE

Andreas Heyden
University of South Carolina
63 PUBLICATIONS **2,645** CITATIONS
SEE PROFILE

Donna Chen
University of South Carolina
59 PUBLICATIONS **1,236** CITATIONS
SEE PROFILE

Adsorbate-Induced Changes in the Surface Composition of Bimetallic Clusters: Pt−Au on TiO_2(110)

Samuel A. Tenney,[†] Jay S. Ratliff,[†] Christopher C. Roberts,[†] Wei He,[†] Salai C. Ammal,[‡] Andreas Heyden,[‡] and Donna A. Chen*[,†]

Department of Chemistry and Biochemistry and Department of Chemical Engineering, University of South Carolina, Columbia, South Carolina 29208, United States

Received: September 18, 2010

The growth, surface composition, and chemical activity of bimetallic Pt−Au clusters on TiO_2(110) have been investigated. Scanning tunneling microscopy (STM) experiments demonstrate that the deposition of Au on Pt clusters results in the formation of bimetallic Pt−Au clusters due to the seeding of the mobile Au atoms at existing Pt nuclei. The composition of the top surface layer of the clusters was studied by low energy ion scattering (LEIS) for bulk compositions ranging from 25%−87.5% Pt with total metal coverages of 0.25 and 0.50 ML. For both coverages, the cluster surfaces consisted of nearly pure Au at Pt compositions of 50% and lower; however, a mix of Au and Pt atoms were found at the cluster surfaces at higher fractions of deposited Pt. These results are consistent with bulk thermodynamics, which predicts a Pt core−Au shell structure based on the lower surface free energy of Au compared to Pt and the large bulk miscibility gap for the two metals. The adsorption of CO on the Pt−Au clusters at room temperature promotes the diffusion of Pt to the surface of the clusters, and this phenomena is most pronounced for the clusters that are initially pure Au at the surface. Density functional theory calculations demonstrate that it is thermodynamically favorable for Pt to diffuse to the cluster surface in order to bind to CO. In contrast, the extent of CO_2 production via sequential adsorption of O_2 and CO on the Pt−Au clusters reflects the surface Pt content before adsorption. For CO oxidation, the first step in the reaction is the dissociation of O_2 at Pt sites. Since this process requires more than one contiguous Pt site, it is not surprising that O_2 dissociation cannot occur on the Pt−Au clusters that are ∼100% Au at the surface before CO exposure, given the low probability for ensembles of Pt sites to form at the surface.

Introduction

The ability to tailor active sites for specific desired reactions has long been a goal for the design and development of superior catalysts. To this end, bimetallic surfaces have shown great promise as novel catalytic materials since bimetallics are known to exhibit properties that are distinctly different from the single metal constituents.[1−5] Recent studies have also demonstrated that the cluster-support interface can play a major role in the chemistry of supported metal clusters, particularly for Au on reducible oxide supports like titania.[6−12] The ultimate goal of this work is to provide fundamental understanding on how the catalytic activity can be tailored through the control of bimetallic surface sites and interactions between the clusters and the support.

Pt−Au bimetallic clusters on TiO_2(110) have been chosen as a model system to explore these concepts of catalytic design on the nanoscale. From a chemical perspective, the Pt−Au bimetallic surfaces have exhibited unusual catalytic properties such as enhanced selectivity for the isomerization and cyclization of *n*-hexane[13,14] and enhanced activity for the dehydrogenation of cyclohexene and cyclohexane to benzene[15,16] compared to pure Pt. More recently, Pt−Au clusters have been reported to be excellent electrooxidation catalysts for potential use in methanol fuel cells since Au inhibits poisoning of Pt sites by species such as CO.[17−19] The presence of Pt in the bimetallic clusters also suppresses cluster sintering,[20] which is a potential problem when the catalysts are heated in air in order to remove residual carbon species.[21] Furthermore, the Pt−Au system is interesting to study because Au and Pt undergo qualitatively different interactions with the titania support: Pt clusters become encapsulated by reduced titania upon heating in ultrahigh vacuum (UHV)[20,22−25] or in H_2[26−28] while Au clusters do not encapsulate.[29] Thus, clusters with both Pt and Au at the surface should have encapsulation behavior that scales with the fraction of Pt and Au at the surface.

Additional chemical interest in the Pt−Au on titania system stems from the unique catalytic properties of Au nanoclusters on titania for propylene oxidation[11,30] and CO oxidation.[10,12,21] In probing the origins of the high activity of Au nanoclusters compared to bulk Au, recent theoretical studies proposed that the active site is at the Au−titania interface.[9] Further experimental support for this proposal is provided by the Rodriguez and Hrbek group, which has demonstrated high activity for the water gas shift reaction on inverse catalysts consisting of titania clusters on Au.[6]

In this work, we have examined the growth and surface chemistry of bimetallic Pt−Au clusters vapor-deposited on TiO_2(110). The TiO_2 support is ideal for these studies since the (110) surface is thermally stable below 1100 K, and the crystal can be made semiconducting for XPS, LEIS, and STM experiments by heating in UHV to preferentially remove oxygen from the crystal. Scanning tunneling microscopy studies confirm

* To whom correspondence should be addressed. Phone: 803-777-1050. Fax: 803-777-9521. E-mail: chen@chem.sc.edu.
[†] Department of Chemistry and Biochemistry.
[‡] Department of Chemical Engineering.

10.1021/jp108939h
Published on Web 11/22/2010

the formation of bimetallic clusters via the deposition of Au onto existing Pt clusters. The surface composition of the bimetallic clusters was examined by low energy ion scattering experiments, which show that the cluster surfaces are nearly 100% Au for bulk Au compositions of >50%. However, adsorption of CO or methanol on the Pt−Au clusters induces the diffusion of Pt to the surface of the clusters. In contrast, CO oxidation does not occur at the cluster surfaces that are initially pure Au; this is presumably because the first step in the oxidation process is O_2 dissociation, which requires neighboring Pt sites.

Experimental Section

Experiments were carried out on a rutile TiO_2(110) crystal (1 cm × 1 cm × 0.1 cm, Princeton Scientific Corp.) in two ultrahigh vacuum (UHV) chambers, which have been described in detail elsewhere.[20,31−34] The base pressures in both chambers were below 1×10^{-10} Torr. Low energy ion scattering (LEIS) and scanning tunneling microscopy (STM) experiments were conducted in the first chamber, which is equipped with a fine focus ion gun (Omicron, ISE100) and hemispherical analyzer (EA125) for LEIS investigations, a variable-temperature STM (Omicron, VT-25), an X-ray photoelectron spectroscopy system that uses the same hemispherical analyzer, a quadrupole mass spectrometer (Leybold Inficon Transpector 2), four-grid optics for low energy diffraction and Auger electron spectroscopy (Omicron, SPEC3), and a load lock assembly.[20,31,32] The second chamber houses a quadrupole mass spectrometer (Hiden HAL 301/3F), which was used for all of the temperature programmed desorption (TPD) experiments, as well as a cylindrical mirror analyzer (Omicron) and low energy diffraction optics (Specs).[33,34]

The TiO_2(110) crystals were cleaned by Ar^+ bombardment (1 kV) for 20 min, followed by annealing at 1000 K for 5 min. The cleanliness of the surface was confirmed by a combination of STM, XPS, LEIS, and Auger electron spectroscopy, depending on which techniques were available in each chamber; (1 × 1) LEED patterns were observed after sputtering and annealing. The crystals were mounted on Ta backplates with Ta foil straps, and the temperature was measured with a type C or type K thermocouple spot-welded to the backplate. The thermocouple readings were independently calibrated using an infrared pyrometer.[31]

In the first chamber, deposition of Pt and Au was achieved with a four-pocket electron beam evaporator (Oxford Applied Research EGCO4). In the second chamber, Au was deposited by passing current through tungsten wire wrapped around a pure Au pellet, and Pt was deposited from a Pt rod using a commercial electron beam evaporator (Omicron, EFM3). In all cases, the metal flux was measured with a quartz crystal microbalance (Inficon), which had been independently calibrated.[20] One monolayer (ML) is defined with respect to the packing densities of the Pt(111) or Au(111) surfaces, which are 1.50×10^{15} atoms/cm^2 and 1.40×10^{15} atoms/cm^2, respectively. Pt fluxes were 0.06−0.1 ML/min in all chambers, and the Au flux was also ∼0.1 ML/min unless otherwise specified. All metal depositions occurred with the sample at room temperature.

LEIS spectra were acquired using a 600 eV He^+ beam at a scattering angle of 130°, a step size of 0.2 eV and a dwell time of 0.2 s. During the 5 min required for the collection of LEIS spectra, changes in Au or Pt intensity due to damage from the He^+ bombardment were less than 10%. STM experiments were conducted at a sample bias of +1.5 V and tunneling current of ∼0.1 nA using electrochemically etched tungsten tips.[20]

The quadrupole mass spectrometer used for TPD studies was enclosed in a stainless steel shroud capped by a gold-plated, moveable flag with a 4 mm diameter round aperture cut in the flag. The crystal was placed approximately 1 mm from the aperture during TPD experiments in order to minimize contributions from desorption from the sample holder. The crystal was also biased at −100 V to prevent electron induced desorption arising from electrons emitted by the mass spectrometer filament. A linear temperature ramp of 2 K/s was generated using an in-house LabView program interfaced with a power supply (Kepco ABC 10−10DM) that provided current to the filament heater. The thermocouple signal was passed through a signal conditioner (Analog Devices 5B401−2) to remove the bias voltage and amplify the signal by a factor of 100.

For CO, O_2, and methanol adsorption experiments, the crystal was positioned approximately 2 mm from the end of a stainless steel direct dosing tube. The chamber pressure was increased by 3.0×10^{-10} Torr for 3 min during exposure to CO (National Welders, 99.99%). For the CO oxidation experiments, the surface was first exposed to oxygen (Matheson, 99.9%) at a chamber pressure of 1×10^{-8} Torr for 5 min followed by CO at 3.0×10^{-10} Torr for 3 min at room temperature.

Computational

Periodic density functional theory (DFT) calculations were performed within the generalized gradient approximation (GGA) using the Vienna ab initio simulation package (VASP).[35−38] Projector augmented-wave (PAW) potentials optimized for the Perdew−Burke−Ernzerhof (PBE)[39] functionals were used to represent the effective potential due to the ionic cores. A (2 × 2 × 1) Monkhorst−Pack *k*-mesh with the energy cutoff of 400 eV was used for all structural relaxations. Energies were calculated with a (5 × 5 × 2) *k*-mesh. The Methfessel−Paxton method[40] of order one with a smearing of 0.2 eV was used to allow for partial occupancy near the Fermi level. Dipole and quadrupole corrections to the total energy were computed using a modified version of the method due to Makov and Payne.[41] The metal (111) surface was modeled by a [3 × 3] supercell with a four-layer slab thickness and a vacuum spacing of 15 Å. The convergence criterion for both electronic and ionic optimization was set to 1×10^{-4} eV. The atoms in the bottom layer of the slab model were fixed to the bulk position of the metal atoms of this layer (usually Au except for pure Pt calculations) and all other atoms were allowed to relax to minimize the total energy; thus, the equilibrium lattice constant for bulk Au (4.17 Å) calculated with the PBE functional and a Monkhorst−Pack *k*-point grid of 11 × 11 × 11 was used for all bimetallic calculations. Pt−Au bimetallic structures were obtained by replacing the Au atoms with Pt atoms at various positions. Finally, the *d*-band center is defined for this paper as the center of gravity of the occupied *d*-band (integration up to the Fermi level) for the nine surface atoms.

Results

Scanning Tunneling Microscopy Studies. STM experiments indicate that for 0.25 ML of Au deposited on 0.25 ML of Pt at room temperature, the Au atoms nucleate at the existing Pt clusters rather than forming new pure Au clusters. STM images of the 0.25 ML Pt clusters before and after deposition of 0.25 ML of Au are shown in Figure 1. Although it was not possible to collect exactly the same regions before and after Au deposition, an analysis of the cluster densities indicates that new clusters are not formed after the addition of Au. The cluster density for 0.25 ML Pt is $1.09 \pm 0.02 \times 10^{12}$ clusters/cm^2 while the density for 0.25 ML Pt + 0.25 ML Au is slightly lower at $9.00 \pm 0.4 \times 10^{12}$ clusters/cm^2. Cluster densities for each surface

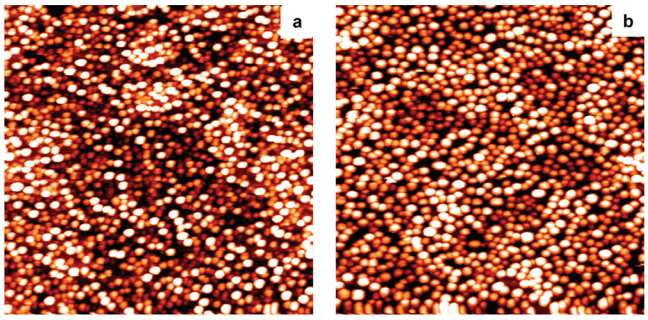

Figure 1. Scanning tunneling microscopy images for the following metals deposited at room temperature on TiO_2(110): (a) 0.25 ML of Pt and (b) 0.25 ML Pt followed by 0.25 ML of Au. Both images are 1000 Å × 1000 Å.

were measured by counting the number of clusters from three different images with a total area of ~3.5 × 10^4 nm^2. The lower cluster density after Au deposition is attributed to cluster coalescence, which is typically observed for deposition of larger metal coverages.[20,42] In any case, there is no evidence for an increase in cluster density due to the formation of pure Au particles. In terms of cluster sizes, the larger clusters on the 0.25 ML Pt surface ranged from 8−13 Å in height and 45−50 Å in diameter, while the smaller clusters were 3.5−5.5 Å in height and 30−40 Å in diameter. For the 0.25 ML Pt + 0.25 ML Au surface, the larger clusters were 12.5−18.0 Å in height and 50−65 Å in diameter, while the smaller clusters were 9−13 Å in height and 35−55 Å in diameter. These values were obtained from STM line profiles of 20 representative clusters (10 larger, 10 smaller) on each surface. It should also be noted that cluster diameters are known to be overestimated due to tip convolution effects,[20] and therefore the height is a better representation of cluster size than diameter or volume. The increase in size for both the smaller and larger clusters after Au deposition is consistent with the incorporation of Au into the existing Pt clusters rather than the nucleation of new clusters. A previous study by our group of 0.076 ML of Au deposited on 0.024 ML Pt clusters has also demonstrated nucleation of Au at the Pt seed clusters.[20]

Low Energy Ion Scattering Studies. In order to investigate the surface composition of the bimetallic Pt−Au clusters, LEIS studies were conducted for cluster compositions ranging from 25−75% Au with a total coverage of 0.5 ML (Figure 2). For comparison, the LEIS spectra are shown for 0.5 ML of pure Pt and pure Au. Due to the similar masses of Pt and Au, the peak energies are separated by only 3.8 eV, but it was still possible to distinguish the contributions of Pt from Au by fitting the Pt−Au spectra with a linear combination of the peaks from pure 0.5 ML of Pt and 0.5 ML of Au. It is known that the local environment of the probed atoms and surface morphology can result in subtle changes to the LEIS line shapes;[43] however, these effects apparently are not significant in the Pt−Au clusters since the spectra of the bimetallic clusters can be fit well by the pure Pt and Au peak shapes. The absolute intensity of 0.5 ML of Au spectrum is 40% lower than that of 0.5 ML of Pt, and this difference is attributed to the larger sizes and lower total surface area of the Au clusters compared to Pt, which forms smaller clusters with greater cluster densities.[20] Thick Pt (10 ML) and Au (20 ML) films were deposited using coverages that left no detectable Ti signal in the LEIS spectrum. After correcting the signals for the total surface area of the films, as determined from a numerical integration of the STM images,[32] the LEIS intensity from the Au film was 90% of that from the Pt film. These differences are believed to be within experimental error,

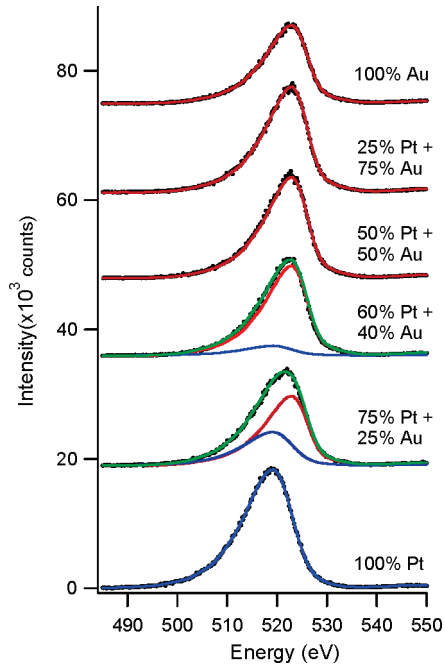

Figure 2. Low energy ion scattering spectra at room temperature for clusters of varying Pt−Au compositions at a total coverage of 0.5 ML. The curve fits for pure Pt are shown in blue and for pure Au are shown in red, while the combined fits are shown in green.

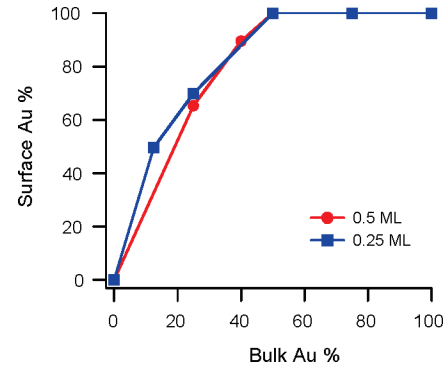

Figure 3. Plot of surface Au % as determined by LEIS, as a function of bulk Au % for clusters with total coverages of 0.5 and 0.25 ML.

indicating that the sensitivities for Pt and Au detection in the LEIS experiment are nearly identical. Therefore, the composition of Au at the surface of the bimetallic clusters was determined from the fraction of total area represented by the pure Au peak in the peak-fit spectra.

The results from this analysis are shown in Figure 3 (circles), which is a plot of the surface composition of Au as determined by LEIS versus the bulk Au composition used in the deposition. For bulk Au compositions of 75% and higher, the surface of the bimetallic clusters is pure Au, and at a 50% composition, the surface is already 100% Au. However, for compositions below 50% Au, it is still possible for Pt to exist at the cluster surfaces. For example, the surface Au composition is 65% for a bulk composition of 25% Au. The presence of exposed Pt at the surface at Au compositions of less than 50% could be attributed to the fact that there is not enough Au to completely cover the Pt clusters. Based on bulk thermodynamics, it is not surprising that the surfaces of the Pt−Au clusters are nearly pure Au for Au compositions above 50%. The lower surface free energy of Au compared to Pt (1.13[44,45] vs 2.48[46] J/m^2) makes it energetically favorable for Au to remain at the surface when Au is deposited on top of Pt. The fact that Au and Pt are

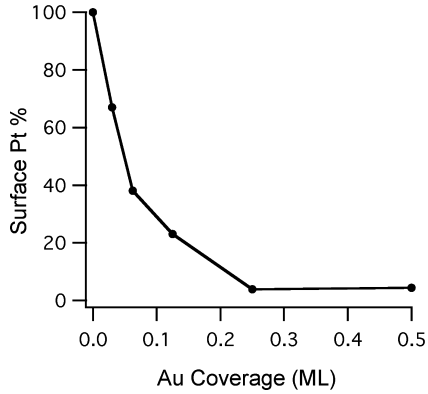

Figure 4. Plot of the Pt at the surface of the bimetallic clusters as determined by LEIS, for 0.25 ML of Pt followed by varying coverages of Au. All data were collected at room temperature.

immiscible at Au compositions greater than 17%[47] also suggests that Au should remain on top of the Pt clusters. Furthermore, atom probe field ion microscopy studies of a bulk Pt−Au alloy containing only 4% Au reported that the surfaces of the alloys were 99% Au after annealing to 873 K, and the Au enrichment extended 4 layers into the bulk with the next three layers being 85, 63, and 25% Au.[48] Similarly, high resolution XPS studies of Pt−2% Au and Pt−15% Au alloys are found to have strong enrichment of Au at the surface.[49] The deposition of Au on Pt is therefore expected form clusters with a shell of Au over a core of Pt if the concentration of Au is high enough to cover all of the Pt atoms at the surface.

Figure 3 also shows the fraction of Au at the surface as a function of bulk Au composition for total coverages of 0.25 ML (squares) that were deposited at the lower flux of 0.01−0.02 ML/min compared to 0.1 ML/min used for the 0.5 ML coverages. If the high surface Au composition is due to kinetic limitations for diffusion into the bulk of the cluster, lower total coverages and deposition rates would be expected to increase the surface Pt content. However, the amount of Au at the surface follows a similar trend to the 0.50 ML coverage, indicating that decreasing the coverage by a factor of 2 does not cause significant differences. In addition, surface compositions were determined for bimetallic clusters formed from the deposition of 0.25 ML of Pt followed by increasing Au coverages up to 0.50 ML (Figure 4). Surface Au compositions of 33%, 62%, 77%, and 100% are observed after deposition of 0.03, 0.625, 0.125, and 0.25 ML of Au, respectively. This result supports the conclusion that Au atoms remain at the surface of the bimetallic clusters after Au deposition although Pt may also exist at the surface when the Au coverage is not high enough to completely cover the surface of the clusters.

For the clusters with a total coverage of 0.25 ML, changes in the Au and Pt signals with heating are shown in Figure 5. The Pt LEIS signal for 0.25 ML of pure Pt does not change appreciably between room temperature and 600 K, but the signal drops to 20% and 3% of the room temperature value after annealing to 800 and 1000 K, respectively (Figure 5a). Since Pt does not desorb from the surface, and the extent of Pt sintering at 1000 K and below is not substantial,[25] the loss in Pt signal is attributed to encapsulation of the Pt clusters by titania. This conclusion is supported by previous studies of Pt on titania demonstrating that Pt is covered by reduced TiO_x after heating in a reducing environment like vacuum[20,22−25] or H_2.[26−28] The Pt−Au clusters that are Pt-rich with 87.5% and 75% Pt exhibit similar decreases in Pt signal upon annealing. The Pt signal drops off less sharply for the Pt−Au clusters compared

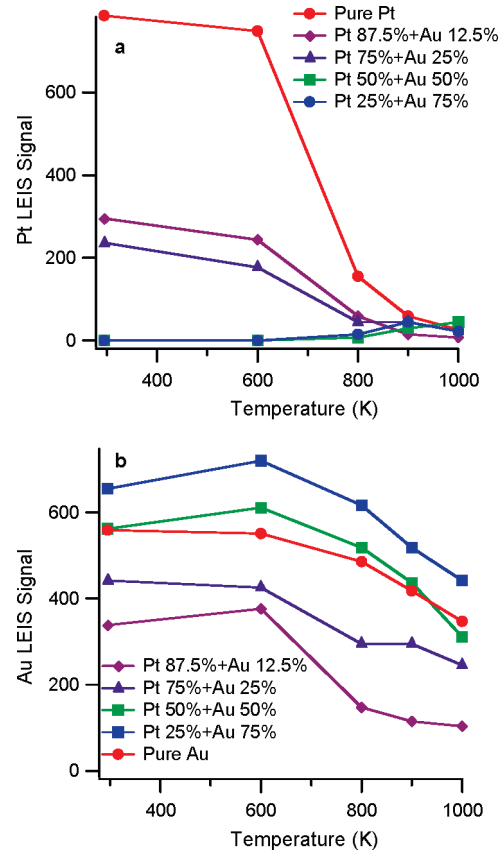

Figure 5. Low energy ion scattering signals for the Pt, Au, and Pt−Au clusters of varying compositions with a total coverage of 0.25 ML: (a) Pt and (b) Au. Surfaces were annealed at each temperature for 1 min.

to pure Pt, but the Pt signal after annealing to 1000 K is still less than 10% of the room temperature value. These results suggest that the presence of large fractions of Au at the cluster surfaces has a minor effect in inhibiting Pt encapsulation, probably because the TiO_x is less likely to migrate onto Au surfaces compared to Pt. For the 50% and 25% Pt clusters, there is initially no Pt signal at room temperature. Surprisingly, the Pt signals increase to nonzero values after heating to 800 K, and at 1000 K, the absolute Pt signals are comparable to those of the pure Pt clusters annealed to the same temperature. The appearance of Pt at the surface of the bimetallic clusters is not well understood. We speculate that it might be related to the formation of Pt−Ti alloys,[50−52] which have been reported for TiO_x films grown on Pt surfaces,[53] but in any case this diffusion of Pt to the surface upon annealing is a small effect. For the pure 0.25 ML Au clusters (Figure 5b), the ∼40% loss in Au signal during heating to 1000 K is attributed to a combination of cluster sintering and Au desorption, which has an onset temperature of 1000 K.[20] Similar changes in Au LEIS signal are observed for all of the Pt−Au bimetallic clusters although the signal drops off slightly more quickly for the Pt-rich clusters between 600 and 800 K. Note that the Au signal intensity is larger for the 75% and 50% Au clusters compared to the pure Au clusters. While the pure Au clusters have the larger total Au coverage, the number of Au atoms residing at the cluster surface is greater for the bimetallics because Pt atoms compose the majority of the bulk of the clusters. Thus, the surface Au signal for the bimetallics remains higher than for the pure Au clusters until the Au composition drops below 50%.

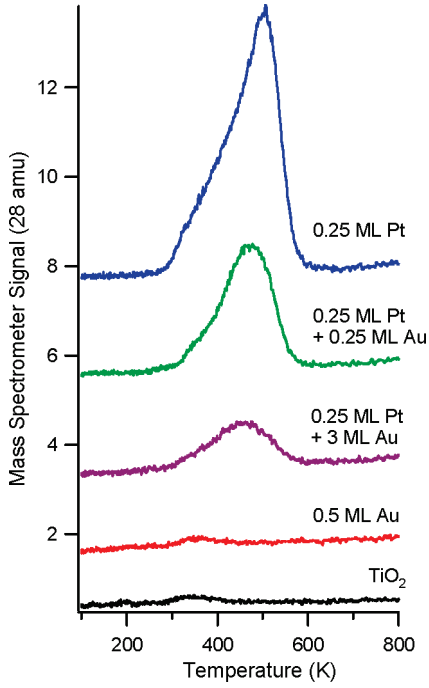

Figure 6. Temperature programmed desorption data for CO adsorbed at room temperature on TiO_2 as well as pure Au, pure Pt and Pt−Au clusters on TiO_2. Surfaces were cooled to 100 K after CO adsorption and then heated at 2 K/s.

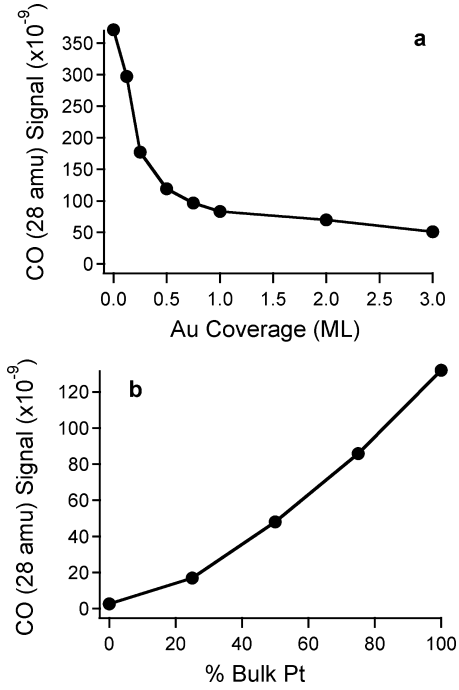

Figure 7. CO desorption yields from TPD of CO on Pt−Au clusters as a function of (a) increasing Au coverage deposited on 0.25 ML of Pt and (b) % Pt composition in clusters with a total coverage of 0.5 ML.

Temperature Programmed Desorption Studies. ***CO Adsorption.*** The desorption of CO was used as a chemical probe to investigate the composition of the Pt−Au clusters. All surfaces were exposed to a saturation dose of CO at room temperature, cooled to 100 K and then heated in front of the shielded mass spectrometer at a rate of 2 K/s. CO desorbs from the pure 0.25 ML Pt clusters with a peak maximum at 500 K, but the onset of desorption occurs just above room temperature, with a low temperature shoulder appearing around 340 K (Figure 6). Little CO adsorbs at room temperature on either the TiO_2 support or the 0.5 ML Au clusters on TiO_2. In both cases, there is a small desorption feature around 350 K with <5% of the integrated intensity for CO on 0.25 ML of Pt. For the bimetallic clusters prepared by depositing various coverages of Au on 0.25 ML Pt clusters, the intensity of the CO desorption peak diminishes with increasing Au deposition; TPD spectra for select Pt−Au clusters are shown in Figure 6, and a plot of integrated CO signal (mass 28 amu) as a function of increasing Au coverage is shown in Figure 7a. Although the general trend of decreasing CO desorption with higher Au coverages is expected, it is surprising that substantial CO signal is still observed on the 0.25 ML Pt + 0.25 ML Au clusters since LEIS studies showed that the surfaces of these clusters are nearly 100% Au. Furthermore, as the Au coverage is increased from 0.25 to 1.0 ML, the CO signal intensity drops from 50% to 20% of the value for pure Pt and remains at roughly 15% even for coverages as high as 2.0 and 3.0 ML of Au. These results suggest that CO induces Pt migration to the cluster surface, allowing CO to bind to Pt atoms even when the surface compositions before adsorption are pure Au.

CO desorption was also investigated for Pt−Au bimetallic clusters with varying compositions and a fixed total coverage of 0.50 ML (Figure 7b) since these surfaces correspond to the LEIS studies in Figure 3. The LEIS experiments demonstrate that surface composition is 100% Au for Pt concentrations at or below 50%. In contrast, for Pt−Au clusters with 50% Pt and 25% Pt compositions, the CO desorption yields are 35% and 15% of that for the pure Pt clusters, respectively. This data provides further evidence for CO-induced migration of Pt to the cluster surfaces. When CO is adsorbed on the 0.25 ML Pt + 0.25 ML Au surface and then heated to 600 K to desorb CO, LEIS experiments show that the surface composition is unchanged from that of 0.25 ML Pt + 0.25 ML Au in the absence of CO. Therefore, if CO induces Pt diffusion to the surface, the Pt atoms must migrate back into the bulk after CO desorption.

Although CO does not stick to pure Au clusters at room temperature, adsorption on both pure Au clusters and the TiO_2 support is observed at 100 K, as shown in the TPD data in Figure 8. On the TiO_2, a sharp CO desorption peak is observed at ~110 K, which is consistent with earlier reported work on CO desorption from ordered TiO_2 thin films on Ru(0001).[54] For the 0.50 ML Au clusters on TiO_2, the sharp 110 K peak is still observed since there is exposed titania at this Au coverage, but the intensity is decreased. Furthermore, a broader peak centered at 175 K appears and is ascribed to CO desorption from Au, as is also observed in CO desorption from Au clusters on titania films.[54] For the pure 0.5 ML Pt clusters, the intensity of the 110 K peak is significantly diminished because much of the surface is covered by the Pt clusters; the desorption peak centered at ~510 K is similar in position and shape to that of CO desorption from pure Pt clusters after room temperature adsorption. Bimetallic Pt−Au clusters consisting of 0.25 ML Pt covered by varying amounts of Au (0.0625−0.5 ML) show a new desorption feature at ~230 K, exhibiting evidence for mixed Pt−Au sites. This peak is most pronounced for the 0.25 ML Pt + 0.25 ML Au clusters, which have the greatest number of potential Pt−Au sites compared to the other bimetallic compositions. On the 0.25 ML Pt + 0.50 ML Au clusters, the low temperature desorption profile more closely resembles that from pure Au since the second desorption maximum is shifted from 230 K back to 175 K, as observed on the Au clusters. However, a higher temperature tail remains from the contribution of CO desorption from Pt−Au. The 230 K feature from Pt−Au

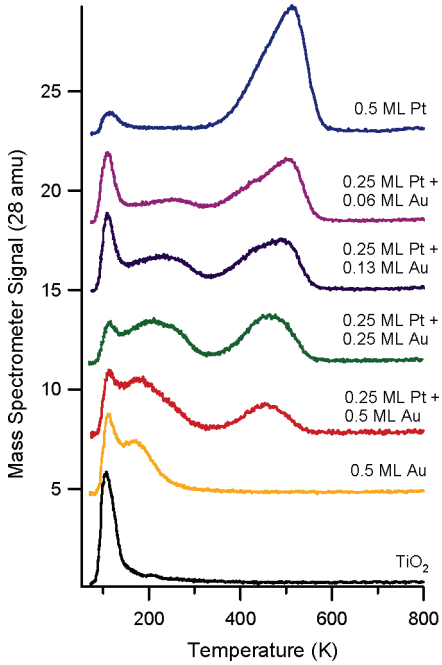

Figure 8. Temperature programmed desorption data for CO adsorbed at 100 K on TiO_2 as well as pure Au, pure Pt and Pt−Au clusters on TiO_2. All temperature ramps were 2 K/s.

is clearly observed at a Au coverage of 0.125 ML, but at 0.0625 ML of Au, this peak is much less apparent, implying that the Au coverage is too low to generate a large number of Pt−Au mixed sites. Similarly, CO desorption from 0.7 ML of Au deposited on Pt(335) exhibits peaks at 190 and 240 K.[55] Both of these features were attributed to adsorption at "alloy" sites, but given that the 190 K peak is also observed on pure Au clusters in the present work, it seems more likely that the 240 K peak is from adsorption at Pt−Au sites, while the 190 K feature is from adsorption at undercoordinated Au sites. These sites are not observed in CO desorption studies on single-crystal Au surfaces.[56,57] In addition, studies of ~1 ML Au deposited on polycrystalline Pt foil show CO desorption peaks at 174 and 237 K, indicative of CO on undercoordinated Au and Pt−Au mixed sites, respectively.[58]

As expected, the intensity of the desorption peak from pure Pt at 510 K is diminished with the addition of Au, as some of the Pt sites become covered. Given that TPD peaks characteristic of desorption from Pt are observed on all of the Pt−Au clusters, these results imply that the CO-induced migration of Pt to the cluster surfaces can occur at relatively low temperatures of <200 K. Notably, the desorption temperature for CO on pure Au clusters on titania films was previously reported to increase with decreasing Au coverage, appearing at 240 K for 0.1 ML of Au and 190 K for 1.5 ML of Au.[54] The shift in desorption temperature was attributed to stronger binding of CO to the monolayer and bilayer islands observed at lower coverages compared to more bulk-like Au at higher coverage. However, the shift to higher desorption temperature observed for decreasing Au content in the Pt−Au studies here is *not* due to a cluster size effect since the clusters sizes are not appreciably different over the coverage range in which the desorption temperature is significantly shifted. It is possible that undercoordinated Au atoms in the bimetallic clusters are responsible for the stronger binding of CO, as has been suggested to explain the stronger CO binding on Au particles supported on other thin oxide films.[59,60]

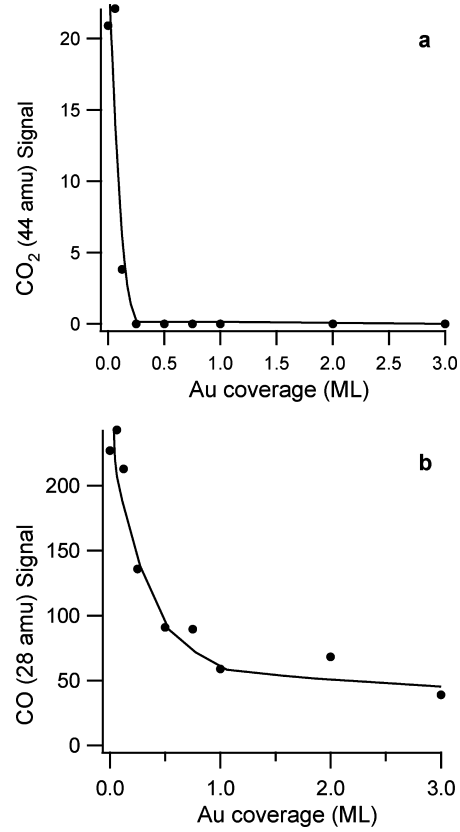

Figure 9. Desorption yields as a function of Au coverage deposited on 0.25 ML of Pt for (a) CO_2 (44 amu) and (b) CO (28 amu). The cluster surfaces were exposed to a saturation dose of O_2 at 300 K followed by CO at 300 K.

Oxidation of CO. The oxidation of CO by preadsorbed atomic oxygen was investigated as a probe reaction on the Pt−Au clusters. In these experiments, the clusters were exposed to a saturation dose of O_2 followed by CO at 300 K. The Pt clusters were exposed to O_2 prior to CO since it is known that adsorbed oxygen does not inhibit molecular CO adsorption on Pt(111) whereas adsorbed CO inhibits O_2 dissociation.[55,61,62] On the 0.5 ML Pt clusters, CO_2 desorption is observed at 425 K along with CO at 515 K. This is consistent with activity on Pt single-crystal surfaces, where O_2 dissociates to atomic oxygen, which then combines with adsorbed CO to produce CO_2.[61−63] Bimetallic Pt−Au clusters were prepared by depositing 0.25 ML of Pt followed by Au coverages varying from 0.0625 to 3 ML, and the CO_2 yield as a function of Au coverage is shown in Figure 9a. CO_2 production falls off sharply with increasing Au coverage, reaching zero at 0.25 ML Pt + 0.25 ML Au, and this decrease in CO_2 production closely follows the trend for surface Pt composition as a function of Au coverage (Figure 4). In contrast, even though the CO evolution decreases sharply up to 0.5 ML of Au (Figure 9b), CO desorption observed from O_2 + CO exposure on the Pt−Au clusters does not drop to zero for Au coverages of 3 ML. On Pt−Au clusters with the same composition, the extent of CO evolution in the O_2 + CO experiments mirrors that of CO desorption from CO adsorption only (Figure 7a). The peak temperature for CO_2 desorption shifts to 400 K for 0.125 ML of Au on 0.25 ML of Pt. Desorption of O_2 is typically observed at ~800 K on Pt(111)[55,61,64] but is not observed on the pure Pt or bimetallic clusters, presumably because oxygen is incorporated into the titania lattice.

Density Functional Theory Calculations. DFT calculations have been carried out on a 4-layer thick slab model representing

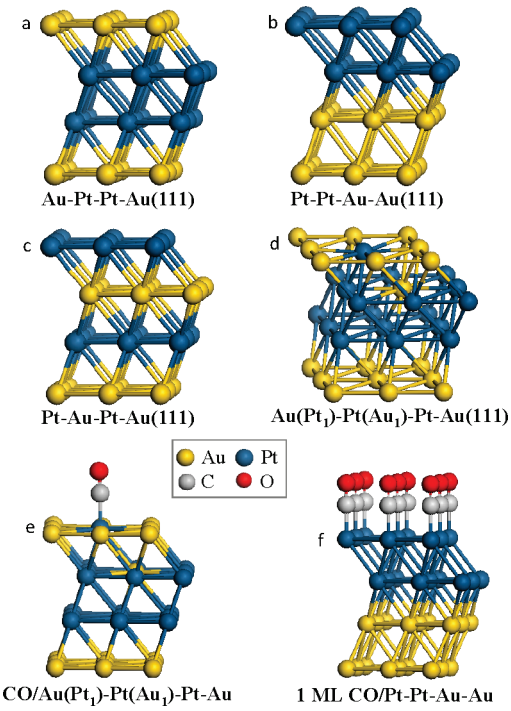

Figure 10. 50% Pt−50% Au 4-layer slab model structures used in the DFT calculations to study bimetallic surfaces: (a) Au−Pt−Pt−Au; (b) Pt−Pt−Au−Au; (c) Pt−Au−Pt−Au; (d) $Au(Pt_1)-Pt(Au_1)-Pt-Au$; (e) the most stable surface structure in the presence of one CO molecule; (f) the most stable surface structure in the presence of 1 ML of CO.

the 50% Pt−50% Au alloy surface, as described in the computational section. Four different surface configurations (Figure 10a−d) were studied by substituting 50% of the Au atoms (18 atoms) with Pt in the 4-layer Au(111) surface model that consists of total 36 atoms. The adsorption of one CO molecule and a monolayer of CO (9 CO molecules) are considered at the atop and 3-fold hollow sites for all surface models investigated. Our calculations predict that an isolated CO molecule prefers to adsorb at the atop position on the Au-terminated surface and at the 3-fold hollow position on the Pt-terminated surface. However, it is likely that on the Pt-terminated bimetallic surfaces the atop site is the preferred adsorption site, contrary to DFT results; it is known that DFT incorrectly predicts CO to adsorb at the 3-fold hollow position on the Pt(111) surface while experiments conclusively show that the atop site is preferred on Pt(111).[65,66] For the adsorption of a monolayer of CO, our DFT calculations again predict the atop position to be preferred for all surfaces. The relative energies (E_{rel}) between the different surface configurations in the presence and absence of CO are summarized in Table 1. The CO adsorption energies (E_{ads}) have been calculated using the equation, $E_{ads}/CO = (E_{surf \cdot nCO} - E_{surf} - nE_{CO})/n$, where $E_{surf \cdot nCO}$ and E_{surf} are the total energies of the surface with and without adsorbed CO molecules, respectively, E_{CO} is the energy of the gas phase CO molecule, and n is the number of CO molecules adsorbed on the surface.

The relative energies of the clean surfaces presented in Table 1 illustrate that the Au-terminated Au−Pt−Pt−Au surface (Figure 10a) is the most stable configuration among the four different surface models considered in the present study. This configuration maximizes the number of strong Pt−Pt bonds and minimizes the number of energetically unfavorable dangling Pt bonds at the surface; dangling Pt bonds are higher in energy than dangling Au bonds as illustrated by the higher Pt surface free energy (2.48 J/m^2 for Pt versus 1.50 J/m^2 for Au).[44−46] For example, the Pt-terminated surfaces, Pt−Pt−Au−Au and Pt−Au−Pt−Au (Figure 10b,c), are less stable than the Au−Pt−Pt−Au configuration by 2.85 and 2.66 eV, respectively. Also, the surface model ($Au(Pt_1)-Pt(Au_1)-Pt-Au$, Figure 10d) constructed by exchanging one surface Au atom with a Pt atom from the second layer in the stable Au−Pt−Pt−Au structure is 0.35 eV higher in energy than the configuration before exchange. These results clearly confirm the experimental observation that the 50% Au−50% Pt alloy surface prefers to form a Au-terminated surface in the absence of adsorbates.

Next, we investigated the effect of low CO adsorption coverage on the energetics of the surface models. The adsorption energies listed in Table 1 illustrate that CO adsorbs more strongly on the surface Pt atoms than on the surface Au atoms. For the adsorption of a single CO molecule on the Au−Pt−Pt−Au surface, it is thermodynamically favorable for a Pt atom from the second layer to exchange with a surface Au atom in order to form a strong Pt−CO bond at the surface (Figure 10e). This result implies that for a Pt−Au system with a surface of pure Au, it is thermodynamically favorable for Pt to diffuse to the surface in the presence of CO, allowing the formation of strong Pt−CO bonds. In the limit of a monolayer CO coverage, all Pt-terminated surfaces are more stable than the Au-terminated surfaces. In particular, the Pt−Pt−Au−Au (Figure 10f) surface was found to be the most stable surface, and this is again consistent with our observation that the CO−Pt/Au system tries to maximize the number of strong Pt−Pt and Pt−CO bonds.

In order to obtain further insights into the adsorption behavior of these surfaces and to test if simple theories, such as the *d*-band theory,[67,68] are able to predict these observations, we calculated the *d*-band center of the four clean surfaces shown in Figure 10a−d. Earlier studies[69−73] have reported that the binding energies for many adsorbates follow a roughly linear relationship with the surface *d*-band center of bimetallic systems, assuming similar structures. Figure 11 shows the CO adsorption energy per molecule for a 1 ML CO coverage versus the *d*-band center for various bi- and monometallic (111) surfaces. It is apparent that the *d*-band theory is able to qualitatively predict the correct ordering of the adsorption strength. CO adsorbs more strongly on systems with a *d*-band center close to the Fermi level such as the Pt-terminated surfaces (Figure 10b,c) and has the weakest adsorption on Au(111), where the *d*-band center is the furthest away from the Fermi level. Also, we observe a nearly linear relationship in adsorption strength versus *d*-band center for all bimetallic systems. Only the pure Pt(111) surface model deviates significantly from this linear relationship, likely because of the different lattice constant used in the Pt(111) model versus all other models. In other words, the linear correlation illustrated in Figure 11 can likely be used in conjunction with simple metal slab calculations to predict whether CO adsorption promotes the diffusion of metal atoms from the bulk to the cluster surface in other bimetallic systems.

Overall, these results are consistent with earlier reports for Pt−Au and Au−Pd alloys in the presence of CO. For example, Song et al.[74] have predicted from DFT calculations of small Pt−Au clusters (≤13 atoms) that CO should induce migration of Pt from the core of the cluster to the surface in order to form strong Pt−CO bonds. Furthermore, Soto-Verdugo and Metiu[75] used DFT calculations to show that CO should induce Pd migration to the surface in Pd−Au alloys due to the stronger binding of CO to Pd as compared to Au.

TABLE 1: Relative Energies (E_{rel} in eV) of Different Configurations of the Pt−Au Surface Models in the Presence and Absence of CO Molecules, as Calculated with the PBE DFT Functional[a]

	Pt−Au, no CO	CO molecule on Pt−Au		One ML of CO on Pt−Au	
	E_{rel} (eV)[b]	E_{rel} (eV)[b]	E_{ads} (eV)	E_{rel} (eV)[b]	E_{ads}/CO (eV)
Au−Pt−Pt−Au (Figure 10a)	0.00	0.00	−0.54	0.00	−0.17
Pt−Pt−Au−Au (Figure 10b)	2.85	1.24/1.31[c]	−2.15/−2.07[c]	−8.37	−1.42
Pt−Au−Pt−Au (Figure 10c)	2.66	1.00/1.40[c]	−2.20/−1.80[c]	−5.83	−1.11
Au(Pt_1)−Pt(Au_1)−Pt−Au (Figure 10d)	0.35	−0.97	−1.86	−0.63	−0.28

[a] E_{ads} (eV) corresponds to the adsorption energy per CO molecule at the atop position except where noted otherwise. [b] The relative energies are calculated with respect to the total energy of the Au−Pt−Pt−Au surface model in each column. [c] The first number corresponds to CO adsorption on the computationally (DFT) preferred 3-fold hollow position and the second number corresponds to the experimentally observed atop position on the Pt atoms.

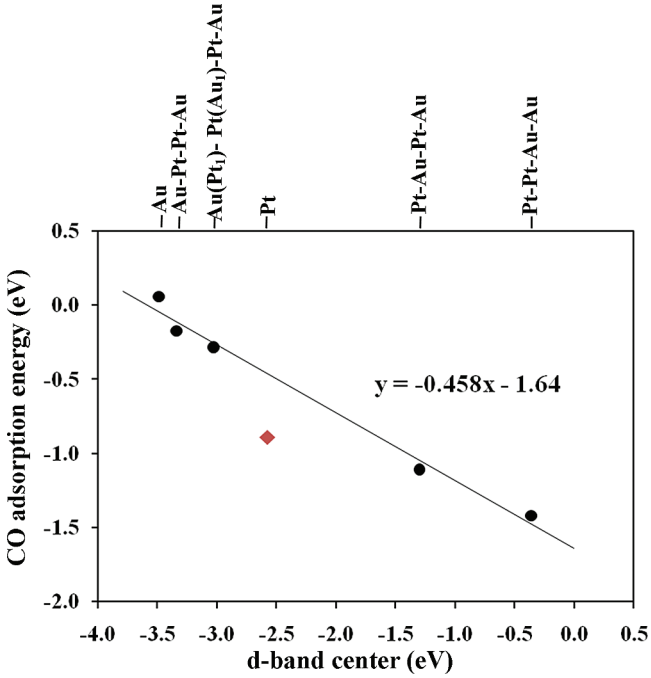

Figure 11. Calculated adsorption energy of one CO molecule on various Pt−Au surfaces with 1 ML CO coverage vs surface *d*-band center. Except for the Pt(111) surface model (red diamond), the lattice constant of Au(111) has been used for all calculations (black dots).

Discussion

Adsorbate-Induced Changes in Surface Composition. The ability of CO adsorption to induce Pt surface segregation in Pt−Au clusters illustrates the dynamic nature of the bimetallic clusters in the presence of adsorbates. Two possible scenarios can explain the desorption of CO from Pt sites on cluster surfaces that are initially pure Au. In the first scenario, diffusion of subsurface Pt atoms is induced by the presence of CO at the surface. In the second scenario, random fluctuations in the surface composition bring Pt atoms to the surface even though the surface composition is on average ∼100% Au. The formation of strong CO−Pt bonds then traps Pt atoms at the surface until the CO is desorbed. Our DFT studies show that it is thermodynamically favorable for CO to bind to Pt at the surface of the Pt−Au system, and therefore, Pt should migrate to the surface if the process if not kinetically limited. Pt atoms in the Pt−Au clusters are apparently able to diffuse to the surface at 240 K, given that CO desorption from mixed Pt−Au sites are observed at these temperatures. Studies in the literature indicate that the Pt atoms should have sufficient mobility at or near room temperature. For example, a CO-induced restructuring of Pt(100) from the "hex" reconstruction to the (1 × 1) surface is observed at 300−340 K.[76−78] Furthermore, the adsorption of CO at room temperature induces lifting of the (1 × 2) reconstruction on Pt(110) to the unreconstructed (1 × 1) surface.[79] Atoms in clusters are also expected to be more mobile than those in the bulk due to the lower coordination numbers for atoms in clusters.

Although there are a number of investigations reporting CO-induced compositional changes in bulk bimetallic alloys and thin films, these changes generally occur at high adsorbate pressures and elevated temperatures. CO does not induce Pt migration to the surface at room temperature for bulk Pt−Au bimetallic surfaces studied in ultrahigh vacuum,[55,58,80] as discussed in a later section on CO desorption. However, a work function study of Pt−Au films showed evidence for Pt diffusion to the surface after several days of exposure to CO at 10^{-4}−10^{-5} Torr at room temperature, and the Pt segregation was accelerated at 473 K.[81] CO on AuPd(100) is a case in which minor diffusion of Pd to the surface is detected even at pressures of 10^{-7} Torr by monitoring the frequency of the C−O stretch in infrared reflection absorption spectroscopy (IRAS) experiments. The AuPd(100) surface is initially ∼100% Au, and after exposure to CO to 180−300 K, a very small peak appears at 2068 cm^{-1} which corresponds to CO binding at Pd atoms that have migrated to the surface.[82] The intensity of this peak increases with CO exposure, becoming much more pronounced at CO pressures of 10^{-5}−10^{-3} Torr.

In contrast to CO, O_2 is an adsorbate that is known to induce changes in the composition of bulk bimetallics at relatively low pressures (10^{-7} Torr) at or near room temperature. An oxygen-induced surface reconstruction of a Cu_3Pt(110) alloy occurs at O_2 pressures of 7.5 × 10^{-9} Torr at room temperature, and segregation of Cu atoms to the surface is also observed.[83] Likewise, the exposure of Cu_3Au(110) to oxygen a room temperature induced Cu segregation to the surface.[84] Tanaka and co-workers reported that bulk $Pt_{0.25}Rh_{0.75}$(100) alloys exposed to O_2 at 10^{-7} Torr temperatures of 400 K or higher induce Rh segregation to the surface, which is driven by the stronger metal−oxygen bond for Rh.[85−89] The same surface segregation of Rh is observed upon exposure to NO, which dissociates into adsorbed oxygen and nitrogen atoms.[85−87,90] In addition, Rh segregation occurs for Pt films deposited on Rh(100) although adsorbate exposure was carried out at higher temperatures of 600−780 K.[89,91]

Supported bimetallic nanoclusters prepared by solution methods also exhibit compositional changes at the surface after high exposures to CO. For example, an infrared spectroscopy investigation of CO on Pt−Au clusters supported on SiO_2 powders suggested that CO binds to Pt at the surface of the clusters at room temperature, based on C−O stretching frequencies, implying that the atoms are mobile within clusters;[92] these Pt−Au clusters were prepared in solution using polyamidoamine dendrimers as stabilizers. Although the composition of the

clusters before CO adsorption could not be analyzed, it was assumed to be pure Au given the lower surface free energy of Au compared to Pt. For Rh_xPt_{1-x} clusters prepared in solution and deposited on Si wafers, exposure to oxidizing (O_2, NO) and reducing (CO, H_2) gases caused reversible changes in the surface composition at 573 K for adsorbate pressures of 100 mTorr.[93,94] Before adsorbate exposure, the surface of the clusters is Pd-rich due to the lower surface free energy for Pd, but during oxidation, the stronger metal-O bond for Rh compared to Pd drives the diffusion of Rh to the surface. In a reducing environment, Rh returns to the metallic state, and Pd diffuses to the surface. Similar behavior was observed for RhPt clusters, where Rh again has a higher surface free energy than Pt, and Rh forms stronger metal−oxygen bonds.[93] However, no change in surface composition was found for PdPt clusters upon exposure to O_2.[93,94] Pd has the lower surface free energy and is more easily oxidized than Pt; consequently, there is no driving force for Pt surface segregation under either oxidizing or reducing conditions. These results are similar to the Pt−Au work reported here in that the metal surface free energies dictate surface composition in the absence of adsorbates, while strong adsorbate-metal bonding drives diffusion of metals to the surface.

In addition, recent work has demonstrated that significant changes in the structure and morphology of bulk Au and Ag surfaces occur at or below room temperature even for adsorbate pressures $<10^{-7}$ Torr. For example, hexagonally shaped vacancy islands on Au(111) become rounded in shape at 180 K under CO pressures of 5×10^{-9} Torr.[95] Exposure of styrene to the Au(111) herringbone reconstruction induces significant surface restructuring.[96] Similarly, NO_2 was found to lift the herringbone reconstruction on Au(111) at 78 K.[97] Friend and co-workers have shown that many adsorbates, including chlorine,[98] sulfur,[99] SO_2,[100] and atomic oxygen produced by NO_2 dissociation[101] cause large-scale surface restructuring on Au(111); specifically, Au atoms are removed from terraces and are incorporated into the adsorbate overlayer, resulting in a rough surface morphology from the formation of pits and islands. On oxygen-covered Ag(111) surfaces, Madix and co-workers have reported that a similar incorporation of Ag atoms into the adsorbate overlayer occurs when the surface is exposed to SO_2,[102] NO_2,[103] and NH_3.[104] The dramatic restructuring of bulk surfaces implies that the metal atoms are quite mobile at these temperatures. Thus, it is not surprising that diffusion of atoms to the surface of the Pt−Au bimetallic clusters should also be facile and capable of significantly changing surface composition and morphology.

Comparison with Other Pt−Au Systems. In terms of cluster growth, the results reported here are in agreement with a previous investigation by our group involving the growth of Pt−Au clusters on TiO_2(110) at lower total coverages of 0.1 ML.[20] Specifically, both STM studies show that Au clusters can be nucleated at existing Pt clusters, forming bimetallic particles. These investigations are consistent with the higher mobility of Au compared to Pt on the titania surface[105] and the existence of strong metal−metal bonds compared to metal−titania.[106] The earlier work also demonstrates that the deposition of Au followed by Pt leads to the formation of pure Pt clusters rather than Pt nucleation at existing Au clusters.

LEIS experiments for both the 0.1[20] and 0.5 ML bimetallic clusters illustrate that the presence of Au does not prevent migration of TiO_x onto the surface of the Pt−Au clusters. After the Pt−Au clusters are annealed, the extent of Pt encapsulation on the surface of the Pt−Au clusters is similar to that on the pure Pt clusters although there is some evidence that the encapsulation is slightly less extensive on the Pt−Au clusters at 800 K compared to pure Pt. In general, there is comparatively little change in the Au signal at 800 K, other than what can be accounted for by sintering, indicating that Au does not become encapsulated by titania. The fact that cluster encapsulation by TiO_x occurs only at the Pt sites and not at the Au sites implies that annealing the Pt−Au clusters should give rise to a surface consisting of Au and titania sites. The Au−titania interface is believed to be the active site for the unique oxidation chemistry on Au nanoclusters supported on titania;[6,10−12] therefore, the annealed Pt−Au structures could provide oxidation catalysts with a greater number of active sites than the titania-supported Au clusters, where the active sites are limited to the perimeter of the Au clusters. Further investigations of the activity of the annealed Pt−Au clusters are the subject of current work.[107]

The main difference for the 50% Pt−50% Au clusters formed at high (0.5 ML) and low (0.1 ML) total coverages is that the surface composition is a mix of Pt and Au at the lower coverage, reflecting the bulk composition, whereas the surfaces are nearly pure Au at the higher coverage. A possible explanation is that the smaller clusters formed at 0.1 ML (5−10 Å high, data not shown) exhibit different alloying behavior than larger clusters produced at 0.5 ML (9−18 Å high, Figure 1b). In fact, it is known that small clusters have different miscibility properties than the bulk materials, with clusters being more likely to form alloys.[108,109] For example, alloyed nanoclusters of Pt−Au were identified by XRD studies for compositions at which the metals are immiscible in the bulk.[17] These bimetallic clusters are ∼20 Å in diameter and were prepared as colloids by solution methods.

Another possibility is that both coverage regimes favor alloying of the Pt and Au atoms at the surface, but kinetic limitations on the diffusion of atoms within clusters at room temperature result in a pure Au surface for the 0.5 ML clusters, in which a larger number of Au atoms must diffuse into the bulk of the clusters in order for the surface to be a mix of Pt and Au. The latter explanation seems less plausible because previous studies of Pt−Au clusters with a total coverage of 4 ML demonstrate that at room temperature, atoms from the bulk are able to diffuse through 2 ML of Au to reach the surface of the clusters.[110] LEIS investigations of 2 ML Au + 2 ML Pt (Pt on Au) deposited on TiO_2(110) at room temperature show that the surface is ∼50% Au and 50% Pt; at these high coverages, no new clusters of Pt are nucleated upon deposition of Pt, demonstrating that the Pt atoms are incorporated into the existing Au clusters to produce bimetallic particles. Consequently, the presence of Au at cluster surfaces is attributed to diffusion of Au atoms to the cluster surface in order to form the most stable Pt core-Au shell structures. The deposition of 2 ML of Au on 2 ML of Pt (Pt + Au) resulted in cluster surfaces that were 100% Au, implying that this is the most stable surface composition, given the evidence of atom mobility at room temperature from the reverse order of deposition.

Investigations of other Pt−Au bimetallic systems consisting of Au films deposited on Pt or Pt films deposited on Au have reported segregation of Au to the surface as well Pt−Au alloying. For example, STM studies of Pt deposited on Au(111) showed Pt alloying into the surface layer at coverages below 0.03 ML.[80] At high coverages, Pt−Au islands appear as Pt is displaced by Au in the first surface layer. A pseudomorphic first layer is formed, followed by a second layer of pure Pt as the Pt coverage is increased. Linear muffin-tin orbital (LMTO) calculations demonstrated that it is energetically favorable for the Pt islands on Au to be capped by gold rather than having Pt

and Au atoms coexist at the surface.[80] However, limitations in atom diffusion at room temperature prevent this from occurring, leaving the surface a mix of Pt and Au. In comparison with the Pt−Au clusters observed in the present study, the fact that the clusters surfaces are pure Au after deposition of Au on Pt is consistent with the prediction that the surfaces prefer to be capped by Au atoms. Notably, Au films deposited on Pt(111)[111,112] and highly stepped Pt(553)[112] form Pt−Au alloys at temperatures above 800 K as Au diffuses into the Pt surface.

CO Desorption on Pt and Pt−Au. CO desorption on the 0.25 and 0.5 ML Pt clusters is similar to that on single crystal Pt surfaces although the peak temperatures and peak shapes are slightly different. On Pt(111), the CO desorption peak shape is relatively symmetric and the maximum desorption intensity occurs at 400−420 K although a shoulder is detected at ∼500 K in some cases.[61,80,113,114] The lower temperature peak is attributed to desorption from terraces while the ∼500 K peak is assigned to desorption from step sites.[55,61] CO desorption from highly stepped Pt(553)[112] or Pt(335)[55] surfaces exhibits a prominent peak at ∼510 K and is also ascribed to the desorption of CO at steps. Furthermore, when the Pt(111) surface is sputtered and annealed only to ∼600 K prior to CO adsorption in order to introduce a greater number of defect sites, a CO desorption peak at ∼500 K appears in addition to the main peak at 420 K.[80] Therefore, the 500 K desorption feature for both the defective Pt(111) surfaces and the 0.5 ML Pt clusters is attributed to undercoordinated sites such as steps and kinks, which are expected to comprise a larger fraction of the surface on the clusters compared to Pt(111). As the fraction of Au is increased in the Pt−Au clusters, the intensity of the 500 K desorption peak decreases, causing a shift to lower temperatures as well as a more symmetric peak shape for CO desorption. This behavior implies that deposited Au atoms occupy the defect sites on the Pt clusters.

CO desorption from Pt films on Au or Au films on Pt is different from on the Pt−Au clusters because CO does not appear to induce diffusion of Pt to the surface. For instance, heating 1.3 ML of Au on Pt(111) to 600 K causes all of the Pt to diffuse subsurface so that CO desorption associated with Pt sites is no longer observed.[80] In contrast to the Pt−Au clusters, CO does not bind to Pt atoms when the surface is initially pure Au. We take this as evidence for the high mobility of atoms in clusters compared to at bulk surfaces, where Pt is unable to migrate to the surface to bind with CO. Similarly, CO adsorption does not induce the migration of Pt to the surface for ∼1 ML Au films on Pt(335)[55] and Pt foils;[58] no CO desorption occurs at ∼400 K, which is the temperature characteristic of CO desorption from Pt sites. The difference between the Pt−Au clusters and the Au film on Pt is again attributed to the higher mobility of atoms in the clusters due to their lower average coordination numbers compared to atoms in the bulk.

CO Oxidation. In order to better understand CO oxidation on Pt−Au clusters, it is useful to consider this reaction within the context of what is known about CO oxidation on pure Pt. The oxidation of CO on O-covered Pt surfaces has been well studied and is believed to occur via a Langmuir−Hinshelwood mechanism with CO strongly adsorbed to the surface before reaction occurs.[62,63] Specifically, chemisorbed CO diffuses to the less mobile atomic oxygen and reacts to form CO_2, which desorbs immediately. For sequential exposure to O_2 and CO, the first step in the reaction process is the dissociation of O_2 on Pt. Studies report that O_2 dissociation occurs around 140 K although O_2 adsorbs molecularly below this temperature.[115,116] Furthermore, O_2 dissociation on Pt occurs via a precursor mediated process, which involves multiple surface sites.[117−122] Since the chemisorption energy for CO is lower than for atomic oxygen, it is assumed that CO diffuses to the less mobile oxygen atoms,[61,123] and atomic oxygen has limited mobility on Pt below 400−450 K.[61,124] A number of investigations also report that reaction occurs at the boundaries of the adsorbed oxygen domains[61,114,125] via diffusion of CO to the perimeter of these islands.[61] It has been proposed that the CO_2 desorption temperature decreases with decreasing CO adsorption energy.[126] CO adsorbed on terraces is more active for CO oxidation than CO at steps due to the higher mobility of the former, but oxygen dissociation occurs primarily at step or defect sites on Pt.[55]

Desorption temperatures for CO_2 in CO oxidation on the 0.25 ML Pt clusters are ∼100 K higher than on Pt(111). On oxygen-covered Pt(111), the peak temperature for CO_2 evolution is at 300−350 K[61,64,114,127] although temperature shifts are observed as a function of oxygen coverage. CO_2 production from the Pt clusters occurs at 420 K, and does not shift with Pt−Au composition. Thus, the rate of CO_2 formation on the Pt clusters appears to be lower than on bulk Pt surfaces. The higher defect densities on the clusters might limit the ability of CO to migrate to the boundaries of the O islands and decrease the rate of reaction. The activation energy for CO oxidation was proposed to be determined by the adsorption energy of CO such that the most strongly bound CO is oxidized at the highest temperature.[126] Consequently, the CO bound strongly at defect sites on the Pt clusters should be less mobile and is expected to contribute to CO oxidation at higher temperatures than on Pt(111).

In contrast to CO adsorption on Pt−Au clusters, CO oxidation characteristic of reaction on Pt does not occur for the clusters with bulk Pt compositions of 50% or lower. Specifically, it appears that O_2 does not dissociate on the Pt−Au clusters, and therefore subsequent exposure of the surface to CO does not produce CO_2, which is observed in reaction only on the pure Pt clusters. The lack of CO oxidation on the clusters consisting of 100% Au at the surface is attributed to the inability to dissociate O_2 on the Pt−Au clusters. Molecular oxygen does not dissociate on Au surfaces, and investigations of Au on Pt(355) also show that O_2 does not dissociate on Au sites modified by underlying Pt or at mixed Pt−Au sites.[55] Given that dissociation of O_2 requires the participation of more than one surface site,[63,115,118,122,128,129] this would explain why CO oxidation cannot occur on the Pt−Au clusters. First of all, it is unlikely that thermal fluctuations in surface composition would bring more than one Pt atom to the cluster surface at any given time. Second, the adsorption energy of O_2[128] is much weaker than that of CO[130,131](∼0.6 eV vs ∼1.5 eV); O_2 would therefore be less likely to trap Pt atoms at the surface than CO even though the binding of atomic oxygen to Pt (∼3 eV)[128,132−135] is stronger than CO to Pt.

Studies of the activity on Au overlayers deposited on Pt(335) also demonstrate that no oxygen dissociation occurs when Pt is completely covered with Au,[55] implying that electronic modification of Au by Pt does not make Au sites active for O_2 dissociation. Furthermore, a 0.7 ML coverage of Au on Pt decreased the atomic oxygen coverage produced from O_2 dissociation by 90% compared to on clean Pt. This result is not surprising since step sites on Pt are known to be more active than terrace sites for O_2 dissociation, and the Au adatoms preferentially occupy the step sites.[55,136] The large decrease in O_2 dissociation ability on the 0.7 ML Au/Pt(335) surface shows that O_2 is not readily dissociated at Pt−Au sites, and therefore it is likely that isolated Pt sites also cannot dissociate O_2 on the Pt−Au clusters. Although the CO_2 yield is lower on the 0.7

ML Au/Pt surface compared to pure Pt due to the lack of atomic oxygen on the surface, CO_2 production occurs at lower temperatures (<300 K), and isotopic labeling studies prove that the low temperature CO_2 originates from CO initially bound at Pt−Au sites. Consequently, it was proposed that O_2 dissociation occurs preferentially at sites near edges of the Au islands, facilitating reaction between the immobile adsorbed oxygen and the mobile CO initially at Pt−Au sites. In contrast, the CO_2 desorption temperature on the Pt−Au clusters is identical to that on the pure Pt clusters.

Insight into CO oxidation reactions on Pt−Au surfaces can be gained from related work on Au−Pd systems since the mechanism for CO oxidation on Pt(111) is known to be similar to that on Pd(111).[62] On Au−Pd alloy surfaces, O_2 cannot dissociate at isolated Pd sites or Au sites, and dissociation occurs exclusively at contiguous Pd sites.[82,126,137,138] CO oxidation therefore does not occur unless contiguous Pd sites are present to facilitate the dissociation of oxygen. This has been shown to be true for AuPd(100) alloy surfaces,[82,137] as well as Au monolayers on Pd(111),[126] Au−Pd overlayers on Mo(110),[138] and Au−Pd clusters supported on a titania thin film.[138] Pd segregates to the surface of the alloys in high pressures of CO due to the energetically favorable Pd−CO bonding, but at pressures of $<10^{-3}$ Torr,[82] contiguous Pd sites are not formed. We propose that isolated Pt sites are also not capable of O_2 dissociation, explaining the lack of CO_2 production on the Pt−Au clusters that initially have no Pt at the surface.

Summary

Pt−Au bimetallic clusters are produced by deposition of Au on pure Pt seed clusters since the high mobility of Au atoms promotes diffusion to existing Pt clusters rather than nucleation of pure Au clusters. Low energy ion scattering studies show that the surfaces of the Pt−Au clusters are pure Au for bulk Au compositions greater than 50% and total metal coverages of 0.25 and 0.50 ML. Upon exposure to CO, desorption characteristic of binding at Pt sites is observed even for Pt−Au clusters with surfaces that are pure Au, indicating that Pt diffusion to the cluster surface is driven by the formation of strong Pt-CO bonds. The mobility of atoms in the bimetallic clusters are greater than that in the bulk, given that CO-induced diffusion of Pt is not observed for Au films on deposited on Pt single-crystals or foils. The yield of CO_2 produced from oxidation of CO scales with the amount of Pt at the surface of the bimetallic clusters. CO oxidation does not occur in the absence of Pt surface sites since O_2 does not dissociate at Au surface sites, and exposure to O_2 does not promote segregation of Pt to the cluster surface.

Acknowledgment. We gratefully acknowledge financial support from the National Science Foundation (CHE 0845788 and CBET-0932991) and the Department of Energy, Basic Energy Sciences (DE-FG02-07ER15842). A portion of this research was performed with TeraGrid resources provided by the National Center for Supercomputing Applications (NCSA), Louisiana Optical Network Initiative (LONI), and the Purdue University under Grant Number TG-CTS090100. Furthermore, computing resources from the USC NanoCenter, USC's High Performance Computing Group, and the Minnesota Supercomputing Institute for Advanced Computational Research are gratefully acknowledged.

References and Notes

(1) Sinfelt, J. H. *Acc. Chem. Res.* **1977**, *10*, 15.
(2) Sinfelt, J. H. *Bimetallic Catalysts. Discoveries, Concepts, and Applications*; John Wiley and Sons: New York, 1983.
(3) Chen, J. G.; Menning, C. A.; Zellner, M. B. *Surf. Sci. Rep.* **2008**, *63*, 201.
(4) Rodriguez, J. A. *Surf. Sci. Rep.* **1996**, *24*, 223.
(5) Campbell, C. *Annu. Rev. Phys. Chem.* **1990**, *41*, 775.
(6) Rodriguez, J. A.; Ma, S.; Liu, P.; Hrbek, J.; Evans, J.; Perez, M. *Science* **2007**, *318*, 1757.
(7) Liu, P.; Rodriguez, J. A. *J. Chem. Phys.* **2007**, *126*.
(8) Lin, X.; Nilius, N.; Sterrer, M.; Koskinen, P.; Hakkinen, H.; Freund, H. J. *Phys. Rev. B* **2010**, *81*, 153406.
(9) Molina, L. M.; Hammer, B. *Appl. Catal., A* **2005**, *291*, 21.
(10) Haruta, M.; Tsubota, S.; Kobayashi, T.; Kageyama, H.; Genet, M. J.; Delmon, B. *J. Catal.* **1993**, *144*, 175.
(11) Hayashi, T.; Tanaka, K.; Haruta, M. *J. Catal.* **1998**, *178*, 566.
(12) Schubert, M. M.; Hackenberg, S.; van Veen, A. C.; Muhler, M.; Plzak, V.; Behm, R. J. *J. Catal.* **2001**, *197*, 113.
(13) Sachtler, J. W. A.; Somorjai, G. A. *J. Catal.* **1983**, *81*, 77.
(14) Yeates, R. C.; Somorjai, G. A. *J. Catal.* **1987**, *103*, 208.
(15) Sachtler, J. W. A.; Biberian, J. P.; Somorjai, G. A. *Surf. Sci.* **1981**, *110*, 43.
(16) Sachtler, J. W. A.; Somorjai, G. A. *J. Catal.* **1984**, *89*, 35.
(17) Luo, J.; Maye, M. M.; Petkov, V.; Kariuki, N. N.; Wang, L. Y.; Njoki, P.; Mott, D.; Lln, Y.; Zhong, C. J. *Chem. Mater.* **2005**, *17*, 3086.
(18) Luo, J.; Maye, M. M.; Kariuki, N. N.; Wang, L. Y.; Njoki, P.; Lin, Y.; Schadt, M.; Naslund, H. R.; Zhong, C. J. *Catal. Today* **2005**, *99*, 291.
(19) Hernandez-Fernandez, P.; Rojas, S.; Ocon, P.; de la Fuente, J. L. G.; Fabian, J. S.; Sanza, J.; Pena, M. A.; Garcia-Garcia, F. J.; Terreros, P.; Fierro, J. L. G. *J. Phys. Chem. C* **2007**, *111*, 2913.
(20) Park, J. B.; Conner, S. F.; Chen, D. A. *J. Phys. Chem. C* **2008**, *112*, 5490.
(21) Haruta, M.; Date, M. *Appl. Catal., A* **2001**, *222*, 427.
(22) Pesty, F.; Steinrück, H.-P.; Madey, T. E. *Surf. Sci.* **1995**, *339*, 83.
(23) Dulub, O.; Hebenstreit, W.; Diebold, U. *Phys. Rev. Lett.* **2000**, *84*, 3646.
(24) Jennison, D. R.; Dulub, O.; Hebenstreit, W.; Diebold, U. *Surf. Sci.* **2001**, *492*, L677.
(25) Ozturk, O.; Ma, S.; Park, J. B.; Ratliff, J. S.; Zhou, J.; Mullins, D. R.; Chen, D. A. *Surf. Sci.* **2007**, *601*, 3099.
(26) Tauster, S. J. *Acc. Chem. Res.* **1987**, *20*, 389.
(27) Tauster, S. J.; Fung, S. C.; Baker, R. T. K.; Horsley, J. A. *Science* **1981**, *211*, 1121.
(28) Tauster, S. J.; Fung, S. C.; Garten, R. L. *J. Am. Chem. Soc.* **1978**, *100*, 170.
(29) Zhang, L.; Persaud, R.; Madey, T. E. *Phys. Rev. B* **1997**, *56*, 10549.
(30) Haruta, M.; Uphade, B. S.; Tsubota, S.; Miyamoto, A. *Res. Chem. Intermed.* **1998**, *24*, 329.
(31) Park, J. B.; Ratliff, J. S.; Ma, S.; Chen, D. A. *J. Phys. Chem. C* **2007**, *111*, 2165.
(32) Zhou, J.; Ma, S.; Kang, Y. C.; Chen, D. A. *J. Phys. Chem. B* **2004**, *108*, 11633.
(33) Ozturk, O.; Park, J. B.; Black, T. J.; Rodriguez, J. A.; Hrbek, J.; Chen, D. A. *Surf. Sci.* **2008**, *602*, 3077.
(34) Varazo, K.; Parsons, F. W.; Ma, S.; Chen, D. A. *J. Phys. Chem. B* **2004**, *108*, 18274.
(35) Kresse, G.; Furthmuller, J. *Phys. Rev. B* **1996**, *54*, 11169.
(36) Kresse, G.; Furthmuller, J. *Comput. Mater. Sci.* **1996**, *6*, 15.
(37) Kresse, G.; Hafner, J. *Phys. Rev. B* **1993**, *47*, 558.
(38) Kresse, G.; Hafner, J. *Phys. Rev. B* **1994**, *49*, 14251.
(39) Perdew, J. P.; Burke, K.; Ernzerhof, M. *Phys. Rev. Lett.* **1996**, *77*, 3865.
(40) Methfessel, M.; Paxton, A. T. *Phys. Rev. B* **1989**, *40*, 3616.
(41) Makov, G.; Payne, M. C. *Phys. Rev. B* **1995**, *51*, 4014.
(42) Park, J. B.; Ratliff, J. S.; Ma, S.; Chen, D. A. *Surf. Sci.* **2006**, *600*, 2913.
(43) Brongersma, H. H.; Draxler, M.; de Ridder, M.; Bauer, P. *Surf. Sci. Rep.* **2007**, *62*, 63.
(44) Sangiorgi, R.; Muolo, M. L.; Chatain, D.; Eustathopoulos, N. *J. Am. Ceram. Soc.* **1988**, *71*, 742.
(45) Chatain, D.; Rivollet, I.; Eustathopoulos, N. *J. Chim. Phys. Physico-Chim. Biol.* **1986**, *83*, 561.
(46) Jiang, Q.; Lu, H. M.; Zhao, M. *J. Phys.: Condens. Matter* **2004**, *16*, 521.
(47) *Binary Alloy Phase Diagrams*, 2nd ed.; Massalski, T. B., International, A., Okamoto, H., Eds.; ASM International: Materials Park, OH, 1990.
(48) Tsong, T. T.; Ng, Y. S.; McLane, S. B. *J. Chem. Phys.* **1980**, *73*, 1464.
(49) Hornstrom, S. E.; Johansson, L.; Flodstrom, A.; Nyholm, R.; Schmidtmay, J. *Surf. Sci.* **1985**, *160*, 561.

(50) Ringler, S.; Janin, E.; Boutonnet-Kizling, M.; Gothelid, M. *Appl. Surf. Sci.* **2000**, *162*, 190.
(51) Chen, W.; Cameron, S.; Gothelid, M.; Hammar, M.; Paul, J. *J. Phys. Chem.* **1995**, *99*, 12892.
(52) Chen, W. H.; Severin, L.; Gothelid, M.; Hammar, M.; Cameron, S.; Paul, J. *Phys. Rev. B* **1994**, *50*, 5620.
(53) Matsumoto, T.; Batzill, M.; Hsieh, S.; Koel, B. E. *Surf. Sci.* **2004**, *572*, 127.
(54) Zhao, Z.; Diemant, T.; Rosenthal, D.; Christmann, K.; Bansmann, J.; Rauscher, H.; Behm, R. J. *Surf. Sci.* **2006**, *600*, 4992.
(55) Skelton, D. C.; Tobin, R. G.; Lambert, D. K.; DiMaggio, C. L.; Fisher, G. B. *J. Phys. Chem. B* **1999**, *103*, 964.
(56) Outka, D. A.; Madix, R. J. *Surf. Sci.* **1987**, *179*, 351.
(57) Canning, N. D. S.; Outka, D.; Madix, R. J. *Surf. Sci.* **1984**, *141*, 240.
(58) Ren, H.; Humbert, M. P.; Menning, C. A.; Chen, J. G.; Shu, Y. Y.; Singh, U. G.; Cheng, W. C. *Appl. Catal. A-Gen.* **2010**, *375*, 303.
(59) Lemire, C.; Meyer, R.; Shaikhutdinov, S. K.; Freund, H. J. *Surf. Sci.* **2004**, *552*, 27.
(60) Shaikhutdinov, S. K.; Meyer, R.; Naschitzki, M.; Baumer, M.; Freund, H. J. *Catal. Lett.* **2003**, *86*, 211.
(61) Gland, J. L.; Kollin, E. B. *J. Chem. Phys.* **1983**, *78*, 963.
(62) Campbell, C. T.; Ertl, G.; Kuipers, H.; Segner, J. *J. Chem. Phys.* **1980**, *73*, 5862.
(63) Petrova, N. V.; Yakovkin, I. N. *Surf. Sci.* **2005**, *578*, 162.
(64) Szabo, A.; Kiskinova, M.; Yates, J. T. *J. Chem. Phys.* **1989**, *90*, 4604.
(65) Feibelman, P. J.; Hammer, B.; Norskov, J. K.; Wagner, F.; Scheffler, M.; Stumpf, R.; Watwe, R.; Dumesic, J. *J. Phys. Chem. B* **2001**, *105*, 4018.
(66) Hu, Q. M.; Reuter, K.; Scheffler, M. *Phys. Rev. Lett.* **2007**, *98*.
(67) Hammer, B.; Norskov, J. K. *Surf. Sci.* **1995**, *343*, 211.
(68) Hammer, B.; Norskov, J. K. *Nature* **1995**, *376*, 238.
(69) Menning, C. A.; Hwu, H. H.; Chen, J. G. G. *J. Phys. Chem. B* **2006**, *110*, 15471.
(70) Menning, C. A.; Chen, J. G. *J. Chem. Phys.* **2008**, *128*, 164703.
(71) Kitchin, J. R.; Norskov, J. K.; Barteau, M. A.; Chen, J. G. *Phys. Rev. Lett.* **2004**, *93*.
(72) Greeley, J.; Mavrikakis, M. *Nat. Mater.* **2004**, *3*, 810.
(73) Menning, C. A.; Chen, J. G. G. *J. Chem. Phys.* **2009**, *130*.
(74) Song, C. R.; Ge, Q. F.; Wang, L. C. *J. Phys. Chem. B* **2005**, *109*, 22341.
(75) Soto-Verdugo, V.; Metiu, H. *Surf. Sci.* **2007**, *601*, 5332.
(76) Thiel, P. A.; Behm, R. J.; Norton, P. R.; Ertl, G. *J. Chem. Phys.* **1983**, *78*, 7448.
(77) Borg, A.; Hilmen, A. M.; Bergene, E. *Surf. Sci.* **1994**, *306*, 10.
(78) Ritter, E.; Behm, R. J.; Potschke, G.; Wintterlin, J. *Surf. Sci.* **1987**, *181*, 403.
(79) Gritsch, T.; Coulman, D.; Behm, R. J.; Ertl, G. *Phys. Rev. Lett.* **1989**, *63*, 1086.
(80) Pedersen, M. O.; Helveg, S.; Ruban, A.; Stensgaard, I.; Laegsgaard, E.; Norskov, J. K.; Besenbacher, F. *Surf. Sci.* **1999**, *426*, 395.
(81) Bouwman, R.; Sachtler, W. M. H. *J. Catal.* **1970**, *19*, 127.
(82) Gao, F.; Wang, Y. L.; Goodman, D. W. *J. Phys. Chem. C* **2009**, *113*, 14993.
(83) Shen, Y. G.; O'Connor, D. J.; Wandelt, K. *Surf. Sci.* **1998**, *410*, 1.
(84) Morgenstern, K.; Niehus, H.; Comsa, G. *Surf. Sci.* **1995**, *338*, 1.
(85) Tanaka, K. *Surf. Sci.* **1996**, *357*, 721.
(86) Tanaka, K. I.; Sasahara, A. *J. Mol. Catal. A* **2000**, *155*, 13.
(87) Tamura, H.; Tanaka, K. *Langmuir* **1994**, *10*, 4530.
(88) Matsumoto, Y.; Okawa, Y.; Fujita, T.; Tanaka, K. *Surf. Sci.* **1996**, *355*, 109.
(89) Matsumoto, Y.; Aibara, Y.; Mukai, K.; Moriwaki, K.; Okawa, Y.; Nieuwenhuys, B. E.; Tanaka, K. *Surf. Sci.* **1997**, *377*, 32.
(90) Hirano, H.; Yamada, T.; Tanaka, K.; Siera, J.; Nieuwenhuys, B. E. *Surf. Sci.* **1989**, *222*, L804.
(91) Tamura, H.; Sasahara, A.; Tanaka, K. *Surf. Sci.* **1994**, *303*, L379.
(92) Lang, H. G.; Maldonado, S.; Stevenson, K. J.; Chandler, B. D. *J. Am. Chem. Soc.* **2004**, *126*, 12949.
(93) Tao, F.; Grass, M. E.; Zhang, Y. W.; Butcher, D. R.; Aksoy, F.; Aloni, S.; Altoe, V.; Alayoglu, S.; Renzas, J. R.; Tsung, C. K.; Zhu, Z. W.; Liu, Z.; Salmeron, M.; Somorjai, G. A. *J. Am. Chem. Soc.* **2010**, *132*, 8697.
(94) Tao, F.; Grass, M. E.; Zhang, Y. W.; Butcher, D. R.; Renzas, J. R.; Liu, Z.; Chung, J. Y.; Mun, B. S.; Salmeron, M.; Somorjai, G. A. *Science* **2008**, *322*, 932.
(95) Hrbek, J.; Hoffmann, F. M.; Park, J. B.; Liu, P.; Stacchiola, D.; Hoo, Y. S.; Ma, S.; Nambu, A.; Rodriguez, J. A.; White, M. G. *J. Am. Chem. Soc.* **2008**, *130*, 17272.
(96) Baber, A. E.; Jensen, S. C.; Iski, E. V.; Sykes, E. C. H. *J. Am. Chem. Soc.* **2006**, *128*, 15384.
(97) Driver, S. M.; Zhang, T. F.; King, D. A. *Angew. Chem.-Int. Ed.* **2007**, *46*, 700.
(98) Gao, W. W.; Baker, T. A.; Zhou, L.; Pinnaduwage, D. S.; Kaxiras, E.; Friend, C. M. *J. Am. Chem. Soc.* **2008**, *130*, 3560.
(99) Biener, M. M.; Biener, J.; Friend, C. M. *Surf. Sci.* **2007**, *601*, 1659.
(100) Biener, M. M.; Biener, J.; Friend, C. M. *Langmuir* **2005**, *21*, 1668.
(101) Min, B. K.; Deng, X.; Pinnaduwage, D.; Schalek, R.; Friend, C. M. *Phys. Rev. B* **2005**, *72*.
(102) Zhou, L.; Gao, W. W.; Klust, A.; Madix, R. J. *J. Chem. Phys.* **2008**, *128*.
(103) Alemozafar, A. R.; Madix, R. J. *Surf. Sci.* **2005**, *587*, 193.
(104) Guo, X. C.; Madix, R. J. *Surf. Sci.* **2002**, *501*, 37.
(105) Iddir, H.; Ögüt, S.; Browning, N. D.; Disko, M. M. *Phys. Rev. B* **2005**, *72*, 081407R.
(106) Campbell, C. T. *Surf. Sci. Rep.* **1997**, *27*, 1.
(107) Tenney, S. A.; Cagg, B.; Ratliff, J. S.; Levine, M.; He, W.; Chen, D. A. in preparation.
(108) Xiao, S.; Hu, W.; Luo, W.; Wu, Y.; Li, X.; Deng, H. *Eur. Phys. J. B* **2006**, *54*, 479.
(109) Christensen, A.; Stoltze, P.; Norskov, J. K. *J. Phys.-Condesed Matter* **1995**, *7*, 1047.
(110) Tenney, S. A.; He, W.; Ratliff, J. S.; Mullins, D. R.; Chen, D. A. *Top. Catal.* **2010**, accepted.
(111) Kobiela, T.; Moors, M.; Linhart, W.; Cebula, I.; Krupski, A.; Becker, C.; Wandelt, K. *Thin Solid Films* **2010**, *518*, 3650.
(112) Davies, P. W.; Quinlan, M. A.; Somorjai, G. A. *Surf. Sci.* **1982**, *121*, 290.
(113) Ertl, G.; Neumann, M.; Streit, K. M. *Surf. Sci.* **1977**, *64*, 393.
(114) Kostov, K. L.; Jakob, P.; Menzel, D. *Surf. Sci.* **1997**, *377*, 802.
(115) Mainardi, D. S.; Calvo, S. R.; Jansen, A. P. J.; Lukkien, J. J.; Balbuena, P. B. *Chem. Phys. Lett.* **2003**, *382*, 553.
(116) Avery, N. R. *Chem. Phys. Lett.* **1983**, *96*, 371.
(117) Shan, B.; Kapur, N.; Hyun, J.; Wang, L.; Nicholas, J. B.; Cho, K. *J. Phys. Chem. C* **2009**, *113*, 710.
(118) Luntz, A. C.; Grimblot, J.; Fowler, D. E. *Phys. Rev. B* **1989**, *39*, 12903.
(119) Rettner, C. T.; Mullins, C. B. *J. Chem. Phys.* **1991**, *94*, 1626.
(120) Zambelli, T.; Barth, J. V.; Wintterlin, J.; Ertl, G. *Nature* **1997**, *390*, 495.
(121) Outka, D. A.; Stohr, J.; Jark, W.; Stevens, P.; Solomon, J.; Madix, R. J. *Phys. Rev. B* **1987**, *35*, 4119.
(122) Luntz, A. C.; Williams, M. D.; Bethune, D. S. *J. Chem. Phys.* **1988**, *89*, 4381.
(123) Lynch, M.; Hu, P. *Surf. Sci.* **2000**, *458*, 1.
(124) Lewis, R.; Gomer, R. *Surf. Sci.* **1968**, *12*, 157.
(125) Wintterlin, J.; Volkening, S.; Janssens, T. V. W.; Zambelli, T.; Ertl, G. *Science* **1997**, *278*, 1931.
(126) Li, Z.; Gao, F.; Tysoe, W. T. *J. Phys. Chem. C* **2010**.
(127) Yoshinobu, J.; Kawai, M. *J. Chem. Phys.* **1995**, *103*, 3220.
(128) Xu, Y.; Ruban, A. V.; Mavrikakis, M. *J. Am. Chem. Soc.* **2004**, *126*, 4717.
(129) Gross, A.; Eichler, A.; Hafner, J.; Mehl, M. J.; Papaconstantopoulos, D. A. *Surf. Sci.* **2003**, *539*, L542.
(130) Hammer, B.; Morikawa, Y.; Norskov, J. K. *Phys. Rev. Lett.* **1996**, *76*, 2141.
(131) Steininger, H.; Lehwald, S.; Ibach, H. *Surf. Sci.* **1982**, *123*, 264.
(132) Gland, J. L.; Sexton, B. A.; Fisher, G. B. *Surf. Sci.* **1980**, *95*, 587.
(133) Campbell, C. T.; Ertl, G.; Kuipers, H.; Segner, J. *Surf. Sci.* **1981**, *107*, 220.
(134) Eichler, A.; Mittendorfer, F.; Hafner, J. *Phys. Rev. B* **2000**, *62*, 4744.
(135) Jacob, T.; Muller, R. P.; Goddard, W. A. *J. Phys. Chem. B* **2003**, *107*, 9465.
(136) Wang, H.; Tobin, R. G.; Lambert, D. K.; DiMaggio, C. L.; Fisher, G. B. *Surf. Sci.* **1997**, *372*, 267.
(137) Gao, F.; Wang, Y. L.; Goodman, D. W. *J. Am. Chem. Soc.* **2009**, *131*, 5734.
(138) Gao, F.; Wang, Y. L.; Goodman, D. W. *J. Phys. Chem. C* **2010**, *114*, 4036.

JP108939H